Algorithm to compute void statistics for random arrays of disks

M. D. Rintoul and S. Torquato
Princeton Materials Institute and Department of Civil Engineering and Operations Research, Princeton University, Princeton, New Jersey 08540
(Received 24 March 1995; revised manuscript received 26 May 1995)

In many-particle systems, the void space (the space not occupied by the particles themselves) is of great interest because of its rich topological features and because it is key in determining the macroscopic properties of the system. Unfortunately, the complex shape and connectedness properties of the void space make precise measurements of quantities that characterize it very difficult, and such measurements must often be made by crude sampling techniques. In this paper we present a method by which void characteristics in random systems of disks can be calculated exactly, in principle. This procedure allows us to compute with very high precision "void" nearest-neighbor distribution functions over a wide range of disk densities. A comparison of these nearest-neighbor measurements to recent theoretical predictions reveals that the predictions are highly accurate.

PACS number(s): 61.20.−p, 05.20.−y

I. INTRODUCTION

Systems of D-dimensional hard spheres have been of great interest to scientists in modeling a variety of many-particle systems. A major reason for this is that the structure of many-particle systems is primarily determined by repulsive interactions at appreciable densities, irrespective of attractive interactions that may be present. The special case of $D = 3$ has been studied in detail due to its use as a model of liquids [1–3], glasses [4,5], particulate composites [6], and powders [7], to mention a few examples. However, the case of $D = 2$ (hard disks) has also been shown to be of interest as a model of fiber-reinforced composites [8], thin films [9], and other systems in which the particles have a circular cross section when projected onto a plane. The case of disks also provides a means of testing various mathematical formulas that might not be as tractable in higher dimensions. For these reasons, the present paper focuses on characterizing hard-disk as well as overlapping-disk systems.

One aspect of the hard-disk system that is especially interesting is the void region, which is just defined as the region exterior to the space occupied by the disks. While the disk space is easily described by a collection of particle centers and radii, the void region is much more complicated to characterize since there are many length scales associated with it. The description becomes even more complicated if one considers not completely hard disks, but disks with hard cores and regions outside the cores which can overlap (the cherry-pit model [10]), or even completely penetrable disks. In this case, portions of the void space may become disconnected, and one now needs to incorporate this topological information in a description of the void space.

Typical quantities associated with the void space that are of physical interest include the void nearest-neighbor functions [2,11], the number of disconnected void regions, and the precise shape of these void regions. Such quantities have traditionally been calculated using a Monte Carlo sampling method. However, this method works rather poorly when the space to be sampled from is very small. This is often the case when one is studying the void space in a dense system, especially systems in which the particles can partially or completely overlap, or if one is looking at the sites in the void which lie in a shell of distance $r + dr$ around a particle. As an example, consider a sampling trial which has probability of success ϵ. For m trials, the expected number of successes is $m\epsilon$, but the relative error associated with that expectation is $1/\sqrt{m\epsilon}$. For $\epsilon = 10^{-6}$ (not at all unreasonably small), one would require 10^8 samples for the relative error in the calculation to be 10%.

Another reason to study the void space in random systems of particles is that Torquato, Lu, and Rubinstein (TLR) [11] have shown that the *particle* nearest-neighbor distribution functions can be easily related to similar distribution functions for the void quantities. Even if the particle quantities were more relevant to a particular situation, calculation of the void quantities often yields a more accurate result, especially for larger distances. This is due to the fact that there is an inherent limit in the accuracy of the particle functions due to the fact that there is a finite (and often small) number of particles in the system of interest. The void space, however, effectively contains a higher dimensionality of sampling points, and the statistics for the void quantities could possibly be much better than the particle quantities for that reason.

Clearly, a better method than random sampling is needed to study the void spaces associated with these systems. There have been some cases where the void spaces have been approximated by polygons [12] and circles [13], with varying degrees of success, but ideally one would like to be able to calculate quantities associated with the void distribution functions *exactly* given a system of sphere centers and radii. An earlier paper by Hoover *et al.* [14] outlines a means for doing such a calculation, but mentions that it fails in certain situations.

In this paper we present a simple and straightforward

algorithm to *exactly calculate* the void-space features. To illustrate the utility of the algorithm, we compute the aforementioned nearest-neighbor distribution functions for random arrays of disks. Our results are compared to a recently derived set of analytical approximations for the nearest-neighbor distribution functions.

II. CHARACTERIZATION OF THE VOID SPACE

The method described here is an extension of that employed by Speedy and Reiss [15], and is very similar to that used by Hoover *et al.* [14]. However, the area is calculated in a somewhat different way, and an explicit description of the formula used to calculate the area is given.

We will first consider a situation in which the particles could partially or completely overlap, such as the cherrypit [10] model, at very high densities. In this case, the void regions will be completely disconnected and each section of the void will consist of a piecewise continuous closed curve as shown in Fig. 1. This curve can be thought of as a surrounding polygon with curved areas removed at each edge corresponding to a segment of a disk. The area of this figure is very easily calculated by first calculating the area of the polygon, and then subtracting out the various circular segments. The area of the polygon could be calculated by breaking the area up into triangles, but instead we use a theorem of Cartesian geometry which tells us that for a polygon with m vertices at coordinates (x_i,y_i), the area A of the polygon is given by

$$A = \frac{1}{2}\sum_{i=1}^{m}(x_{i-1}y_i - y_{i-1}x_i), \tag{1}$$

where $x_0 = x_m$ and $y_0 = y_m$, and the vertices are taken in order in a counterclockwise direction. If the vertices are taken in a clockwise direction one just gets $-A$. This cannot be directly compared to the method used by Hoover *et al.* [14] since the formula used to compute the area was not explicitly stated.

One can now calculate the area of all of the void regions in this dense system by identifying every edge of a sphere which does not lie inside of another disk and constructing the curves generated by connected sets of these edges. To ensure that you are always traversing the voids in a counterclockwise manner, it is necessary only to store the circular edges in a *clockwise* manner, and then connect up the end of one edge to the beginning of the next.

Now suppose one has a situation as in Fig. 2. In this case, there is an isolated cluster of disks within a void region. However, if we just follow the recipe given above, we will calculate the total area of the void space (as if the inner cluster did not exist) by traversing the edges of the outer shell. We will also construct a curve formed by edges of the inner cluster, only this time if we have been traversing the original disks in a clockwise manner, we will traverse the inner figure in a clockwise manner, and get a negative value for the area. As long as the circular segments also change sign, they will add to the area, instead of subtracting from it. This will be subtracted from the area calculated for the first calculation, and we will be left with the true area of void space, without having to treat that case any differently. This same argument applies to any level of nesting clusters within other clusters. It should be noted that this algorithm will calculate the two disk cluster correctly, since the area of the polygon will be 0, but the two circular segments will add up to be the correct area. Similarly, for one isolated disk, one again gets the correct answer if one considers the segment of the circle to subtend an angle of 2π.

Finally, one needs to consider the boundary conditions associated with the system. Usually, one chooses periodic boundary conditions to best reduce edge effects. If there is one cluster that percolates through the system in both

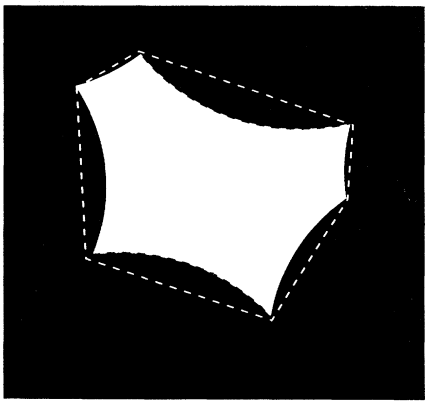

FIG. 1. Sample void (colored white) surrounded by disks (colored black). The polygon formed by the edges is also shown as the white dotted line.

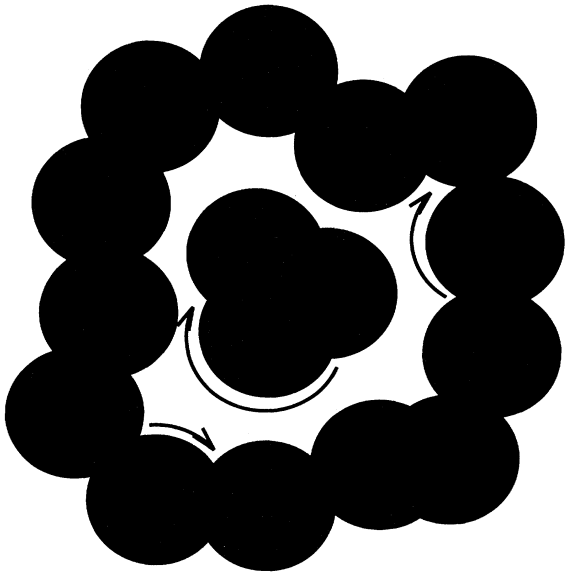

FIG. 2. Example of a cluster of disks contained within a void. The arrows all move around the individual disks in a clockwise direction, and therefore traverse the void and the isolated cluster in different directions.

directions, then the algorithm needs no modifications, as all void space will be bounded by disks. If, however, there is no percolating cluster in either direction, then the algorithm is only calculating the area of all of the clusters, and this total result (which will be negative) must be added to the total area of the box to get the area of the void space.

Percolation in one direction presents a problem, as the segments on each of the clusters that percolate in one direction do not form a closed curve, but instead form two open curves (corresponding to either side of the cluster) which simply move across the box for one box length. In the work of Ref. [14], the simulation simply stopped when this occurred, and, as a result, these authors were unable to get good results for densities when this occurred. We have solved this problem by "cutting" the cluster and having the curve trace through it, and treating this as a nonpercolating case. This is most easily done by identifying the cluster which percolates in one direction (along with the direction) and subjecting it to free boundary conditions in the direction of percolation. Care must be taken in this case to properly keep track of the length and number of the true disk edges. It should also be noted that in the case of periodic boundary conditions one must be sure to use absolute coordinates when measuring the area of the polygon, or the results will be incorrect if a cell boundary is crossed. If free boundary conditions are used, one just needs to be careful to treat the edges which lie along the side of the box differently than the edges which lie along the other disks, if the particles are allowed to overlap the edge. In this paper, only periodic boundary conditions were used.

Using the method described here, one can now calculate any of the void quantities of interest. Not only is the total area known, but the size and shape of all of the individual sections which comprise the void space are also known. Moreover, the total length of all of the edge segments is just the surface area of the void. Knowledge of these values can be used to calculate almost any information that one requires about the void space. It is also important to note that this method can be used for disks with a distribution of radii and not just systems of equal-sized disks, although only the latter is considered here as an example.

III. NEAREST-NEIGHBOR FUNCTIONS: THEORY

As an application of the algorithm, we will calculate precisely the void nearest-neighbor distribution functions $H_V(r)$, $E_V(r)$, and $G_V(r)$ as well as the "particle" nearest-neighbor functions $H_P(r)$, $E_P(r)$, and $G_P(r)$ as defined by Torquato *et al.* for random distributions of disks at number density ρ. We note that the void quantities are identical to the ones first introduced by Reiss, Frisch, and Lebowitz [2] in their scaled-particle theory.

The nearest-neighbor quantities have been defined in any space dimension, but for concreteness we define them for two dimensions as follows.

$H_V(r)\,dr$ = probability that at an arbitrary point in the system the center of the nearest particle lies at a distance between r and $r+dr$, (2)

$H_P(r)\,dr$ = probability that at an arbitrary disk center in the system the center of the nearest disk lies at a distance between r and $r+dr$, (3)

$E_V(r)$ = probability of finding a region which is a circular cavity of radius r (centered at some arbitrary point), empty of disk centers, (4)

$E_P(r)$ = probability of finding a region which is a circular cavity of radius r (centered at some arbitrary disk center), empty of disk centers, (5)

$2\pi r\rho G_V(r)$ = probability that, given a region which is a circular cavity of radius r that is empty of particle centers, particle centers are contained in the shell of area $2\pi r\,dr$ encompassing the cavity, (6)

$2\pi r\rho G_P(r)$ = probability that, given a region which is a circular region of radius r centered on an abitrary disk that is empty of any other particle centers, particle centers are contained in the shell of area $2\pi r\,dr$ encompassing the cavity. (7)

The fraction of the space occupied by the disks is denoted by ϕ. (In the special case of nonoverlapping or hard disks, $\phi = \rho\pi\sigma^2/4$. If the disks can overlap, then $\phi \leq \rho\pi\sigma^2/4$.)

It is important to note that the nearest-neighbor functions have alternative, and useful interpretations. In D dimensions, the value of $E_V(r)$ is just the fraction of space available to a test particle of radius $r-\sigma/2$ inserted into the system, and $H_V(r)$ is just the surface area per

unit volume of the interface between the available and unavailable spaces [11,16]. In two dimensions in particular, E_V and H_V are just the area fraction and perimeter per unit area, respectively, of the portion of the void space that remains when each of the actual disks of radius $\sigma/2$ is surrounded by a disk of radius r. We can divide up this *remaining void space* into distinct connected regions, which we will refer to as "cavities."

For values of ϕ below the value of the percolation threshold of the actual disk system, there will always be one large cavity which percolates through the entire system when the surrounding disk is the same size as the actual disk. [For the special case of the hard-disk system, there will only be one large cavity since the nonoverlap condition forbids the formation of any localized (i.e., disconnected) cavities.] However, as the surrounding disks are added to the actual disks, the surrounding disks begin to form larger connected "clusters," and more parts of the void become disconnected. For large enough values of r, the clusters formed by the surrounding disks will percolate through the system. In two dimensions, this implies that the void system will no longer percolate, and will consist of small, isolated cavities.

We can now define further quantities of interest related to the cavities. Let $n(r)$ represent the average cavity density (number of cavities per unit area) for a system of disks in which each actual disk of radius $\sigma/2$ is surrounded by a disk of radius r. Moreover, let $v(r)$ and $s(r)$ be the average cavity area and perimeter, respectively. We can now write

$$n(r)v(r) = E_V(r), \tag{8}$$
$$n(r)s(r) = H_V(r). \tag{9}$$

For values of r in which a large cavity percolates through the entire system, $v(r)$ and $s(r)$ will be "extensive" quantities. However, as r gets larger, the void region becomes disconnected, and the quantities become "intensive." Speedy [17] has shown that the equation of state for a hard-sphere system in D dimensions can be written in terms of $v(\sigma)$ and $s(\sigma)$.

The nearest-neighbor quantities are all interrelated for D-dimensional sphere systems. The value of $E_{V(P)}(r)$ can be calculated from $H_{V(P)}(r)$ by the formula

$$E_{V(P)}(r) = 1 - \int_0^r H_{V(P)}(x)\,dx, \tag{10}$$

and conversely, one can write

$$H_{V(P)}(r) = \frac{-\partial E_{V(P)}(r)}{\partial r}. \tag{11}$$

Finally, $G_{V(P)}(r)$ can be written in terms of $E_{V(P)}(r)$ and $H_{V(P)}(r)$ as

$$H_{V(P)}(r) = \rho 2\pi r G_{V(P)}(r) E_{V(P)}(r), \tag{12}$$

which allows $E_{V(P)}(r)$ to be written solely in terms of $G_{V(P)}(r)$ as

$$E_{V(P)}(r) = \exp\left(-\int_0^r \rho 2\pi y\, G_{V(P)}(y)\,dy\right). \tag{13}$$

Torquato *et al.* [11] have derived exact series representations of all of the nearest-neighbor quantities for D-dimensional interacting spheres in terms of the probability density $\rho_n(\mathbf{r}_1,\ldots,\mathbf{r}_n)$ which characterizes the probability of finding n spheres with positions $\mathbf{r}_1,\ldots,\mathbf{r}_n$. For general potentials, ρ_n is not obtainable exactly for $n \geq 2$.

A. Overlapping disks

For spatially uncorrelated disks (Poisson distributed centers) or fully overlapping disks (one of the extreme limits of the cherrypit model), $\rho_n = \rho^n$ and the aforementioned series representation can be evaluated exactly [11] as

$$H_{V(P)}(r) = \rho 2\pi r \exp(-\rho\pi r), \tag{14}$$
$$E_{V(P)}(r) = \exp(-\rho\pi r), \tag{15}$$
$$G_{V(P)}(r) = 1. \tag{16}$$

The area fraction ϕ occupied by the overlapping disks is given by

$$\phi = 1 - E_V(\sigma/2) = 1 - \exp\left(-\frac{\rho\pi\sigma^2}{4}\right). \tag{17}$$

B. Hard disks

In the case of hard disks, an exact evaluation of the nearest-neighbor functions is not possible for reasons already given. In the region $r \leq \sigma/2$, the void quantities are known exactly to be

$$E_V(r) = 1 - \rho\pi r^2 \qquad (0 \leq r \leq \sigma/2), \tag{18}$$
$$H_V(r) = \rho 2\pi r \qquad (0 \leq r \leq \sigma/2), \tag{19}$$
$$G_V(r) = \frac{1}{1-\rho\pi r^2} \qquad (0 \leq r \leq \sigma/2). \tag{20}$$

In this case, the area fraction occupied by the disks is given by

$$\phi = 1 - E_V(\sigma/2) = \rho\pi\sigma^2/4. \tag{21}$$

Clearly, in the hard-core regions, the particle quantities are given by

$$E_P(r) = 1 \qquad (0 \leq r \leq \sigma), \tag{22}$$
$$H_P(r) = 0 \qquad (0 \leq r \leq \sigma), \tag{23}$$
$$G_P(r) = 0 \qquad (0 \leq r \leq \sigma). \tag{24}$$

Torquato *et al.* found that for a statistically homogeneous system of D-dimensional hard spheres in equilibrium, the void and particle quantities could be related for $r \geq \sigma$:

$$E_P(r) = \frac{E_V(r)}{E_V(\sigma)} \qquad (r \geq \sigma), \tag{25}$$

$$H_P(r) = \frac{H_V(r)}{E_V(\sigma)} \qquad (r \geq \sigma), \tag{26}$$

and

$$G_P(r) = G_V(r) \qquad (r \geq \sigma). \tag{27}$$

Roughly speaking, an equilibrium distribution of hard spheres is the most random distribution subject to the impenetrability constraint.

Torquato [18] has recently derived approximate expressions for the particle quantities for hard disks in equilibrium in the region $r > \sigma$. Two different sets of relations were derived: one valid up to the *freezing point* [19] and the other valid from freezing up to random close packing. In the present paper we will simulate hard-disk systems up to the freezing point. The analytical expressions [18] that are valid up to freezing are given by

$$G_{V(P)}(x) = a_0 + \frac{a_1}{x} \qquad (x \geq 1), \tag{28}$$

$$E_P(x) = \exp\{-\phi[4a_0(x^2-1) + 8a_1(x-1)]\} \quad (x \geq 1), \tag{29}$$

$$H_P(x) = 8\phi(a_0 x + a_1)E_P(x) \qquad (x \geq 1), \tag{30}$$

where $x = r/\sigma$,

$$a_0 = \frac{1 + 0.128\phi}{(1-\phi)^2}, \tag{31}$$

and

$$a_1 = \frac{-0.564\phi}{(1-\phi)^2}. \tag{32}$$

Analytical approximations for the void quantities $E_V(r)$ and $H_V(r)$ can also be calculated from Eqs. (12), (13), and (28) with the results

$$E_V(x) = (1-\phi)\exp\left[-\phi(4a_0x^2 + 8a_1x + a_2)\right] \qquad (x > \tfrac{1}{2}), \tag{33}$$

$$H_V(x) = 8\phi(1-\phi)(a_0x + a_1) \times \exp\left[-\phi(4a_0x^2 + 8a_1x + a_2)\right] \qquad (x > \tfrac{1}{2}), \tag{34}$$

where

$$a_2 = -(a_0 + 4a_1). \tag{35}$$

Similarly, one can also test the above particle nearest-neighbor functions by measuring the void quantities and scaling the measured values of $E_V(r)$ and $H_V(r)$ by $E_V(\sigma)$.

IV. SIMULATION DETAILS

In order to test the previous analytical expressions it is necessary to simulate systems of equilibrium disks and measure either the void or particle quantities. For small values of ϕ, this can be done via sampling methods. However, Monte Carlo (MC) sampling [20] has the disadvantage mentioned previously that the error associated with the result goes as $m^{-1/2}$, where m is the number of samples. This decreases very slowly as a function of m. Also, the value of $E_V(x)$ [or $E_P(x)$] becomes very small very quickly for $x \geq 1$ as ϕ becomes larger. This causes the sampling method to become prohibitively time consuming in this region. This is especially relevant for the calculation of $G_{V(P)}(x)$ as the factor of $E_{V(P)}(x)$ appears in the denominator of the expression for $G_{V(P)}(x)$ as a function of $E_{V(P)}(x)$ and $H_{V(P)}(x)$. It is important to be able to test these expressions for large values of ϕ since this is the more difficult region to describe theoretically. In this region, the impenetrability condition is expected to play the largest role.

The values of $E_V(r)$ and $H_V(r)$ can be easily obtained via the algorithm described earlier by the physical interpretation of the two quantities as being the area fraction and perimeter per unit area of the void space remaining when the actual disk centers are surrounded by disks of radius r. One can now get the full range of values for r by surrounding the actual disks with larger and larger circles, measuring the void space, and repeating until no voids remain.

In the case of totally hard disks, data were generated for each value of ϕ in the following manner. First, disk centers were laid down on a cell (with periodic boundary conditions) without regard to overlap. Then, each disk was chosen sequentially and checked to see if it overlapped other disks. If it did overlap, attempts were made to move it to reduce overlap. If it did not overlap, an attempt was made to move it using a MC type algorithm, which the nonoverlapping condition strictly enforced. This was done until there was no overlap, and then the entire system was equilibrated using a MC procedure, where the step size was chosen to make the acceptance rate close to 50%. There were 10 000 steps per particle attempted during the equilibration procedure. We chose to use the random starting points (without regard to overlap) rather than melting a crystal since some of the densities used were close to the freezing density, and we have noticed that correlations associated with the initial crystal structure can persist after very long time scales.

After the system was equilibrated, $E_V(r)$, $H_V(r)$, $n(r)$, $v(r)$, and $s(r)$ were measured for the system, and the system was then evolved using the MC algorithm described previously with 50 steps per particle attempted. This procedure was repeated with those same quantities being measured after each set of MC evolutions. Finally, these procedures were averaged over many different initial configurations. The values calculated for $G_V(r)$ are calculated from the final average of $H_V(r)$ and $E_V(r)$, and

TABLE I. Simulation parameters used for each value of ϕ. In the table, N is the number of particles in each sample. Each configuration was evolved for 50 MC move attempts per particle between samples.

ϕ	N	Samples per configuration	Configurations
0.30	10000	50	15
0.50	5000	50	25
0.65	5000	50	50

TABLE II. Theoretical and measured values of $E_V(r)$ for the case of fully penetrable (Poisson distributed) disks, where $\phi = 1 - \exp(-0.5) \approx 0.393$.

r/σ	$E_V(r)$ theory	Measured	Difference
0.100000	0.980198673	0.980195141	3.5315×10^{-6}
0.500000	0.606530660	0.606582577	-5.1917×10^{-5}
1.000000	0.135335283	0.135780606	-4.4532×10^{-4}
1.500000	0.011108996	0.011309312	-2.0032×10^{-4}
2.000000	0.000335462	0.000364083	-2.8621×10^{-5}

are not an average over a $G_V(r)$ calculated for each individual configuration. Specific values of the parameters for each value of ϕ are given in Table I. The corresponding particle quantities were also calculated at the same time that the void quantities were calculated. However, in this case only $H_P(r)$ was calculated. This was done by binning the nearest-neighbor distance associated with each particle in the system. Then, $E_P(r)$ was calculated by numerically integrating $H_P(r)$ after all of the data for $H_P(r)$ had been collected. Then $G_P(r)$ was calculated from $H_P(r)$ and $E_P(r)$.

The nearest-neighbor void quantities were also measured for fully penetrable disks. In this case, 50 configurations of 5000 particles were used, with no equilibration. $E_V(r)$ and $H_V(r)$ were measured for each configuration, and then averaged over the 50 configurations. The value of $G_V(r)$ was then calculated from the final values of $E_V(r)$ and $H_V(r)$.

The accuracy of the method was checked in three different ways. First, the void quantities were also measured using random sampling techniques, and found to give values similar to the ones computed with the method described above. Also, regular arrangements of disks in which the answers were analytically known were also measured, and the values were found to correspond to the analytical values (up the the precision of the computer). These regular arrangements included disks which did not percolate, percolated in one direction, and percolated in both directions. Finally, $E_V(r)$ was also calculated for selected random systems by using Eq. (10) and integrating the values of $H_V(r)$ which are easily computed. This was compared to the direct measurement of $E_V(r)$ and found to be very close.

V. RESULTS

A. Fully penetrable spheres

Since the theoretical results for the fully penetrable system are exactly known, the only discrepancies between the measured data and the theory should be due to fluctuations associated with choosing the random particle centers and finite size effects from the periodic boundary conditions. Thus this model serves as an excellent benchmark to test the accuracy of our algorithm. For the 5000 particle system, the effects of the periodic boundary conditions should be very small, and the statistical fluctuations associated with averages over many 5000 particle systems should also be small. Table II shows a theoretical and measured value for $E_V(r)$ for various values of r, where the reduced number density of spheres is given by $\rho\pi\sigma^2/4 = 0.5$. This corresponds to a disk area fraction of $\phi = 1 - \exp(-0.5) \approx 0.393$. The extreme precision of the measured results was a further confirmation that the method worked properly.

B. Comparison to the theoretical predictions

We give nearest-neighbor results for hard disks in equilibrium here. The data are checked against Eqs. (28), (33), and (34) to test their accuracy. Figure 3 shows the results for $E_V(r)$ plotted along with Eq. (33) against r/σ. The theoretical prediction gives a very good approximation to the measured values, even for large values of r and ϕ. A magnified version of this plot is shown in Fig. 4, showing the accuracy of the prediction for the larger values of r. The measured values of $H_V(r)$ are plotted along with the theoretical values from Eq. (34) in Fig. 5 and these too show a very strong agreement.

The case of $G_V(r)$ is more interesting and is shown in Fig. 6. Although the simulation results and the theory results match very closely for $\phi = 0.30$ and $\phi = 0.50$, the value of $G_V(r)$ for $\phi = 0.65$ is significantly different

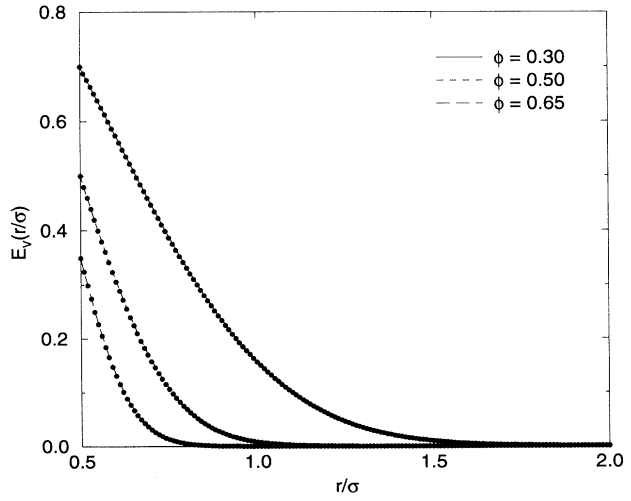

FIG. 3. Equation (33) (shown as lines) compared to simulation values of $E_V(r)$ (shown as points) for various values of ϕ.

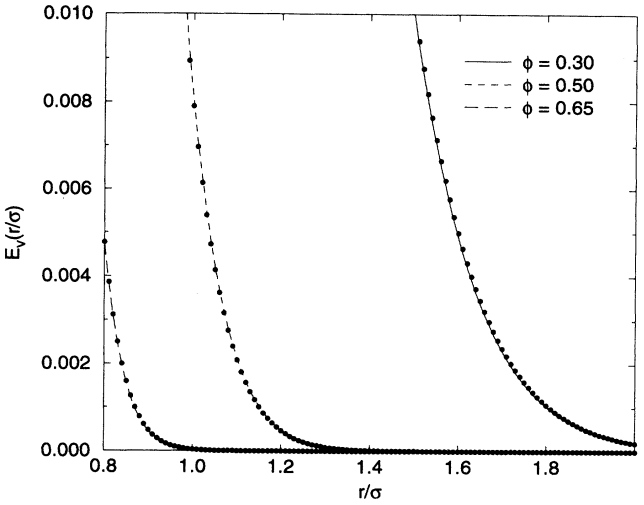

FIG. 4. Same as Fig. 3, except that the y axis is greatly enlarged to show details for larger values of r.

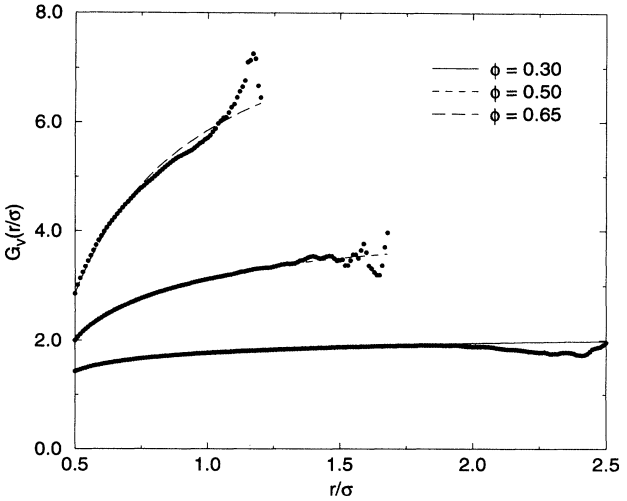

FIG. 6. Equation (28) (shown as lines) compared to simulation values of $G_V(r)$ (shown as points) for various values of ϕ.

than the theoretical prediction for values of $r > \sigma$. This is due to the fact that in the simulations there are a statistically insignificant number of voids which contain areas that lie more than a distance of σ away from the nearest particle center (or equivalently, the area in which one could insert a test particle of radius $\sigma/2$); $G_V(r)$ examines the rate of change of the size of these voids. In this case, $G_P(r)$, which is equivalent to $G_V(r)$ for $r > \sigma$, is a better quantity to measure in the simulations.

C. Comparison of void and particle quantities

Figure 7 shows a plot of $E_P(r)$ and $E_V(r)/E_V(\sigma)$ for $r \geq \sigma$. A close look at the data shows that although the equality of Eq. (25) clearly holds for these values, the data for $E_V(r)$ generally show much less fluctuation. This was also true in comparisons of $H_P(r)$ versus $H_V(r)/H_V(\sigma)$ and $G_P(r)$ versus $G_V(r)$. The particle quantities have the disadvantage that there are larger fluctuations in the data due to the relatively small number of sample points associated with each system. Furthermore, these points must be "binned" and are subject to the normal errors associated with the binning process. This points out an example of how the void statistics can be used to more accurately determine quantities related to the particle statistics.

D. Average density, area, and perimeter of voids

The average number of cavities per unit area, $n(r)$, is plotted in Fig. 8 as a function of the size of the surround-

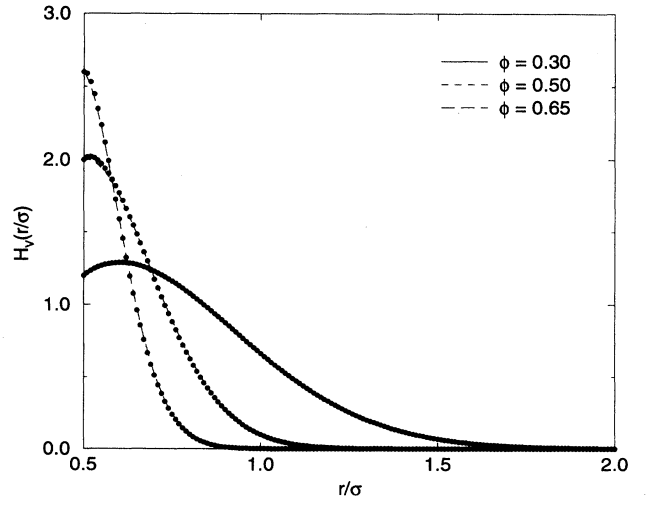

FIG. 5. Equation (34) (shown as lines) compared to simulation values of $H_V(r)$ (shown as points) for various values of ϕ.

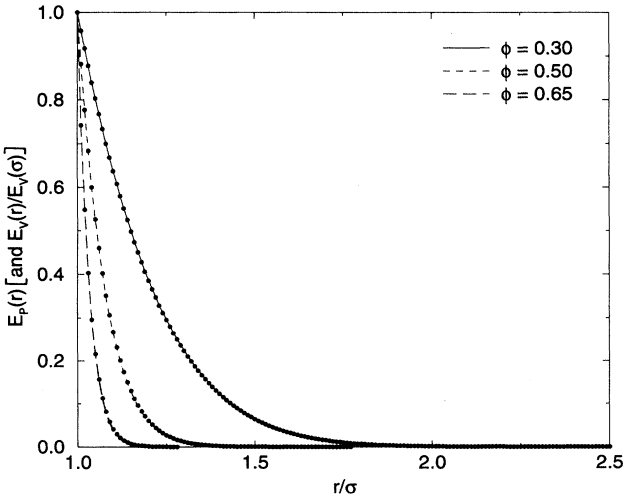

FIG. 7. Simulation values of $E_P(r)$ (shown as lines) and of $E_V(r)/E_V(\sigma)$ (shown as points) for various values of ϕ.

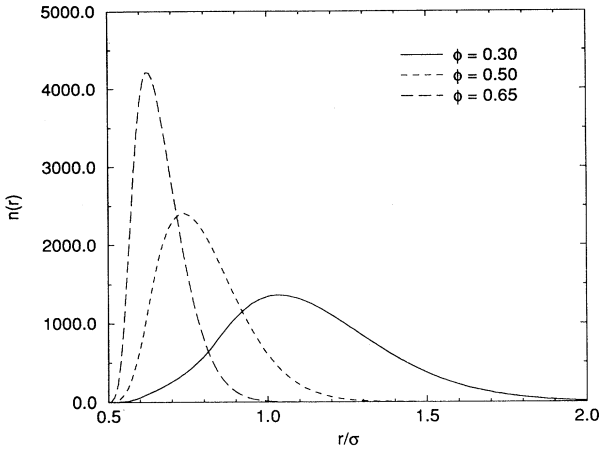

FIG. 8. Simulation values of $n(r)$ for a system of unit area and 5000 disks.

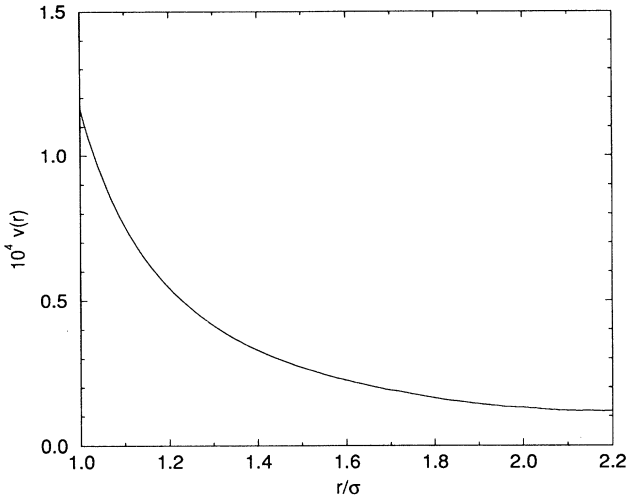

FIG. 9. Simulation values of $v(r)$ for a system of unit area and 5000 disks for $\phi = 0.30$. Only the region where $v(r)$ is intensive is shown, i.e., area fractions above the percolation threshold of the equivalent cherrypit system [21,22].

ing imaginary disk. This quantity increases very sharply for the densest system as the largest void quickly breaks up into many smaller voids. Figure 9 shows the behavior of $v(r)$ as a function of the ratio of the surrounding disk of radius r to the actual disk radius $\sigma/2$, in the region where the void does not percolate and $v(r)$ is intensive. The percolation threshold was calculated for each system by comparing it to the equivalent cherrypit model [21,22], and calculating the threshold for that model. The graph shown is shown only for $\phi = 0.3$, since the scales for each of the three different densities are significantly different. However, all three values of ϕ show the same qualitative behavior. Although we obtained $v(r)$ through a direct calculation, it could have also been obtained from $E_V(r)$ (Fig. 3) and $n(r)$ via relation (8). Similarly, the perimeter $s(r)$ can now be obtained from the results given in Fig. 8 and our results for $H_V(r)$ (Fig. 5).

VI. CONCLUDING REMARKS

We have explicitly described a method by which void statistics in random disk systems can be calculated exactly. By using this method, we are able to greatly improve the precision with which most quantities related to the void space can be measured. Furthermore, we are able to compute precisely nearest-neighbor correlation functions associated with the void space and show that important nearest-neighbor particle functions can be measured more precisely by studying the void quantities. Although the examples presented here consisted of equal-sized disks, the method can be completely generalized to disks having any size distribution.

The calculation of the nearest-neighbor quantities is just one example of the utility of the numerical technique presented here. The algorithm can be applied as well to compute (1) the precise shape and number of sides of cavities in the hard-disk equilibrium system; (2) corresponding void statistics for the nonequilibrium random-sequential-addition process [13] for hard disks; and (3) void characteristics of experimental systems such as monolayers of small colloidal systems. We plan to address all of these issues in future papers.

[1] J. P. Hansen and I. R. McDonald, *Theory of Simple Liquids* (Academic Press, New York, 1986).
[2] H. Reiss, H. L. Frisch, and J. L. Lebowitz, J. Chem. Phys. **31**, 369 (1959).
[3] Y. Song, R. M. Stratt, and E. A. Mason, J. Chem. Phys **88**, 1126 (1988).
[4] B. J. Alder and T. E. Wainwright, J. Chem. Phys **33**, 1439 (1960).
[5] R. Zallen, *The Physics of Amorphous Solids* (Wiley, New York, 1983).
[6] S. Torquato and F. Lado, Phys. Rev. B **33**, 6428 (1986).
[7] M. Shahinpoor, Powder Technol. **25**, 163 (1980).
[8] S. Torquato and F. Lado, Proc. R. Soc. London, Ser. A **417**, 59 (1988).
[9] T. I. Quickenden and G. K. Tan, J. Colloid. Interface Sci. **48**, 382 (1974).
[10] S. Torquato, J. Chem. Phys. **81**, 5079 (1984); **84**, 6345 (1986).
[11] S. Torquato, B. Lu, and J. Rubinstein, Phys. Rev. A **41**, 2059 (1990).
[12] K. S. Sturgeon and F. H. Stillinger, J. Chem. Phys. **96**, 4651 (1992).
[13] J. Feder, J. Theor. Biol. **87**, 237 (1980).
[14] W. G. Hoover, N. E. Hoover, and K. Hanson, J. Chem. Phys. **70**, 1837 (1979).
[15] R. J. Speedy and H. Reiss, Mol. Phys. **72**, 1015 (1991).
[16] S. Torquato, J. Stat. Phys. **45**, 843 (1986).
[17] R. J. Speedy, J. Chem. Soc. Faraday Trans. II **76**, 693 (1980); **77**, 329 (1981).
[18] S. Torquato, Phys. Rev. E **51**, 3170 (1995).

[19] The freezing density described here represents the density at which the fluid-solid transition has been reported to occur. Although there is no mathematical proof of its existence, there are many analytical and simulation results which strongly support its existence at a numerical value of $\phi \approx 0.69$ (see Refs. [23,24]). Above the freezing point, the fluid (or disordered) state can persist along the metastable branch which is conjectured to end at the random close packing value of about 0.82 [25].

[20] M. P. Allen and D. J. Tildesley, *Computer Simulation of Liquids* (Clarendon Press, Oxford, 1987).

[21] S. B. Lee and S. Torquato, J. Chem. Phys. **89**, 3258 (1988).

[22] S. B. Lee and S. Torquato, J. Phys. A **41**, 5338 (1990).

[23] W. G. Hoover and F. H. Ree, J. Chem. Phys. **49**, 3609 (1968).

[24] J. Tobochnik and P. M. Chapin, J. Chem. Phys. **88**, 5824 (1988).

[25] J. Berryman, Phys. Rev. A **27**, 1053 (1983).